



Figures and figure supplements

T-ALL leukemia stem cell 'stemness' is epigenetically controlled by the master regulator SPI1

Haichuan Zhu *et al*

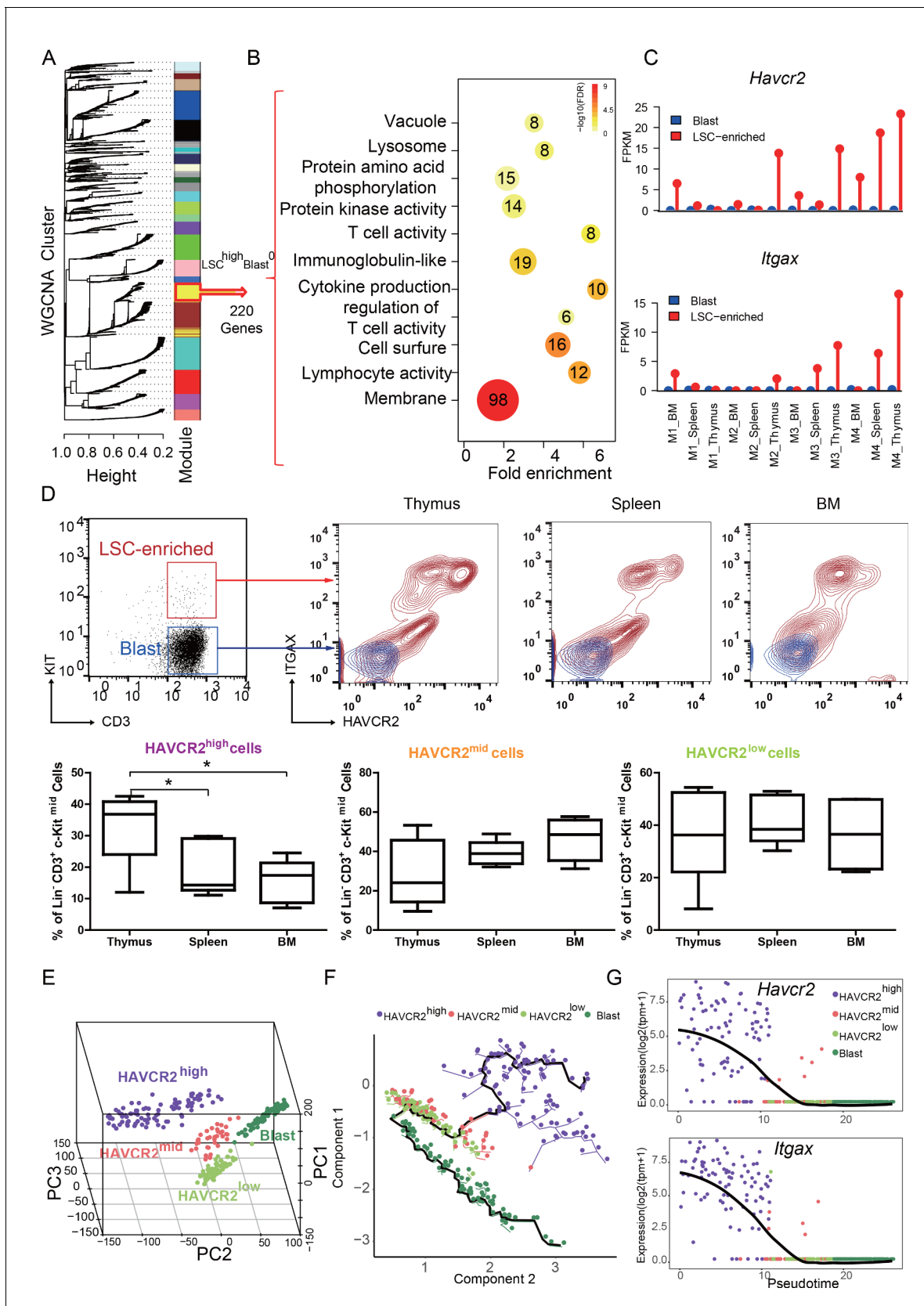


Figure 1. HAVCR2 redefines a heterogeneous LSC-enriched subpopulation at single-cell resolution (A) WGCNA analysis for the bulk RNA-seq of LSC-enriched and leukemic blast subpopulations. The yellow module contains 220 genes that are preferentially expressed in the LSC-enriched subpopulation. Figure 1 continued on next page

Figure 1 continued

subpopulation (LSC^{high}-Blast⁰); (B) Gene Ontology (GO) analysis of LSC-enriched genes in the yellow module; (C) *Havcr2* and *Itgax* are specifically expressed in LSC-enriched (red) but not in leukemic blast (blue) subpopulations isolated from the indicated hematopoietic organs of M1-M4 *Pten*-null T-ALL mice; (D) Upper panel: FACS plots are overlaid to show the differential expression of HAVCR2 and ITGAX in the LSC and blast subpopulations. The previously defined Lin⁻CD3⁺KIT^{mid} LSC-enriched subpopulation (in the red box in the left panel) can be further separated into several subgroups based on the expression of the cell-surface markers HAVCR2 and ITGAX. The Lin⁻CD3⁺KIT⁻ leukemic blast subpopulation (in the blue box in the left panel) does not express HAVCR2 or ITGAX. Lower panel: Quantitative measurement of the HAVCR2^{high}, HAVCR2^{mid} and HAVCR2^{low} subgroups in different hematopoietic organs from *Pten*-null T-ALL mice (n = 5; *, p<0.05). The HAVCR2^{high} subgroup is enriched in the thymus; (E) PCA analysis of the single-cell transcriptome shows four subgroups, labeled in different colors. Cells from two independent mice are indicated by different shapes; (F) Pseudotime analysis shows the expression profiles of T-ALL cells in 2-D component space. The solid black line shows the main differentiation path from HAVCR2^{high} (purple) to blasts (dark green); (G) Pseudotemporal ordering of single cells based on *Havcr2* or *Itgax* expression. BM: bone marrow.

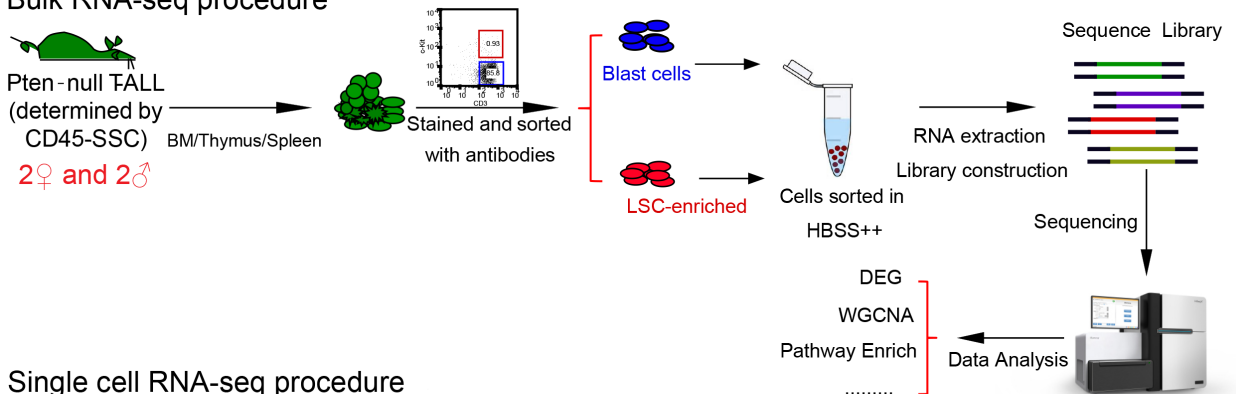
DOI: <https://doi.org/10.7554/eLife.38314.002>

A

Cell Type	LSC-enriched		blasts
initiating	Yes		No
MYC	30% low	70% high	100% high
Rapamycin	resistance	sensitive	sensitive
JQ1	resistance	sensitive	sensitive
BrdU	Low	high	high
Surface marker	KIT ^{mid}		KIT ⁻

B

Bulk RNA-seq procedure



Single cell RNA-seq procedure

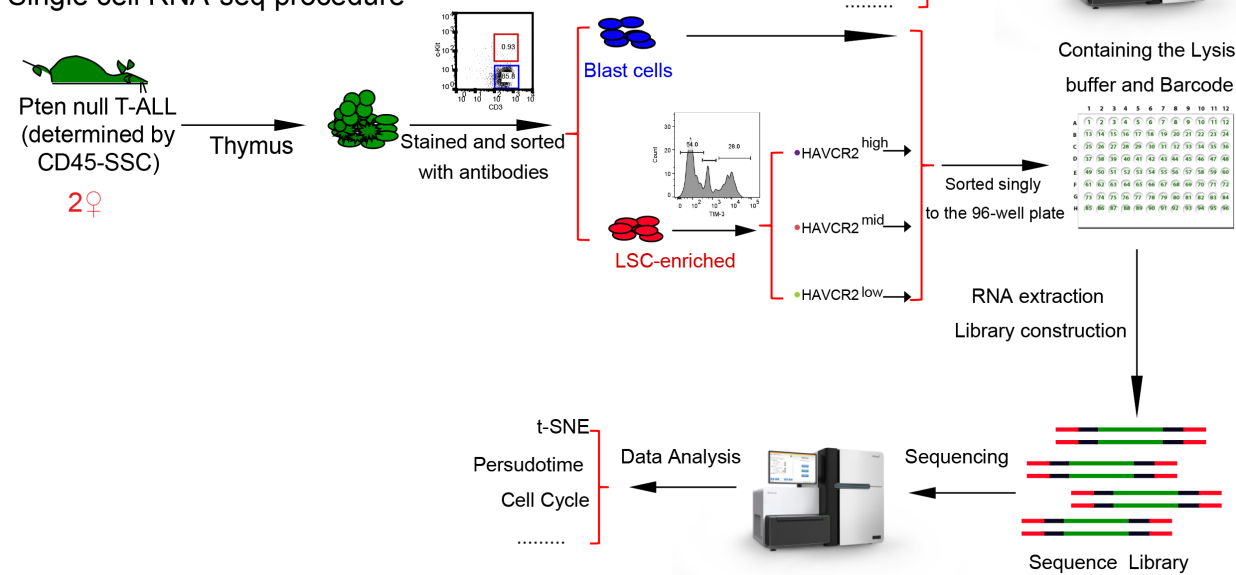


Figure 1—figure supplement 1. A schematic illustration of procedures used for Bulk and single cell RNAseq analysis. (A) Heterogenous properties of LSC-enriched and leukemic blast subpopulations. (B) Schematic illustrations of the procedures used for the isolation of LSC-enriched and leukemic blast subpopulations and the bulk (upper panel) and single-cell (lower panel) RNA-seq analyses.

DOI: <https://doi.org/10.7554/eLife.38314.003>

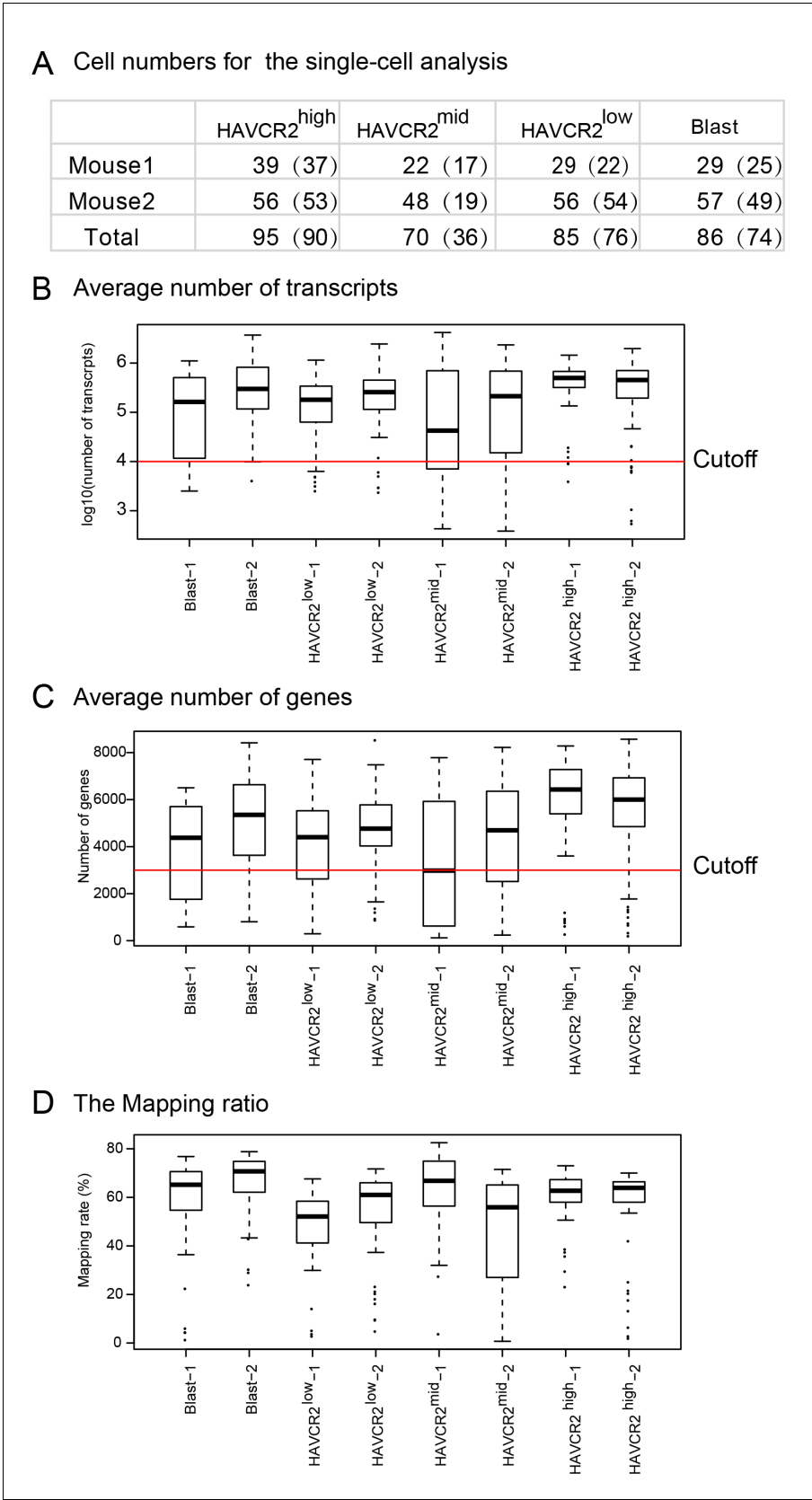


Figure 1—figure supplement 2 continued

used for further analyses; (B–C) Boxplots of the average numbers of transcripts (B) and genes (C) detected in each subgroup; (D) Mapping ratio of the raw reads in each subgroup.

DOI: <https://doi.org/10.7554/eLife.38314.004>

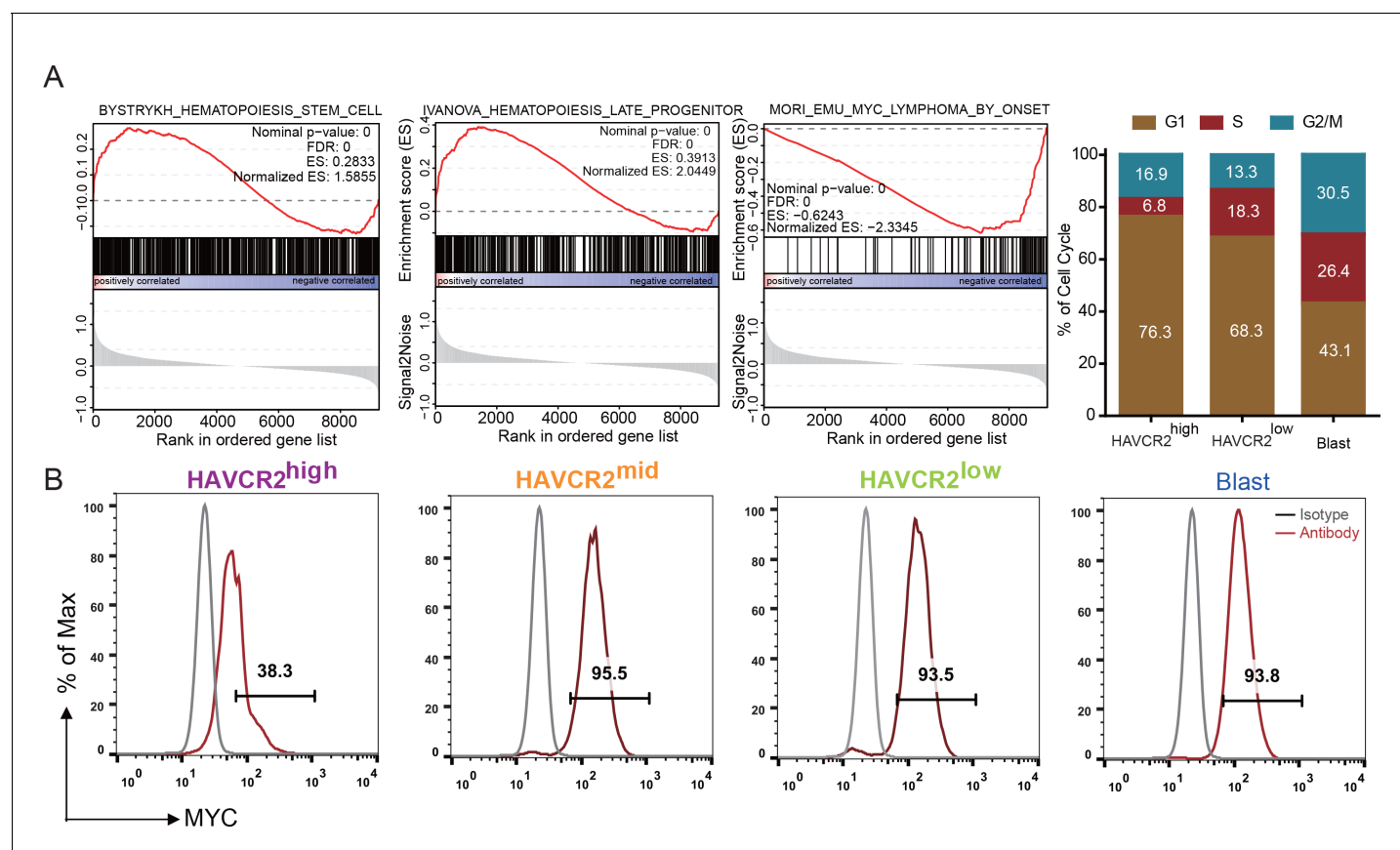


Figure 2. Cells in the HAVCR2^{high} subgroup are in a quiescent cell cycle state. (A) Left panel: GSEA analysis shows signaling pathways enriched in the HAVCR2^{high} and blast subpopulations. Right panel: Percentage of cells in each phase of the cell cycle based on single-cell RNA-seq; (B) Intracellular FACS analyses of MYC levels in the HAVCR2^{high}, HAVCR2^{mid}, HAVCR2^{low} and blast subgroups. Gray line: isotype control.

DOI: <https://doi.org/10.7554/eLife.38314.005>

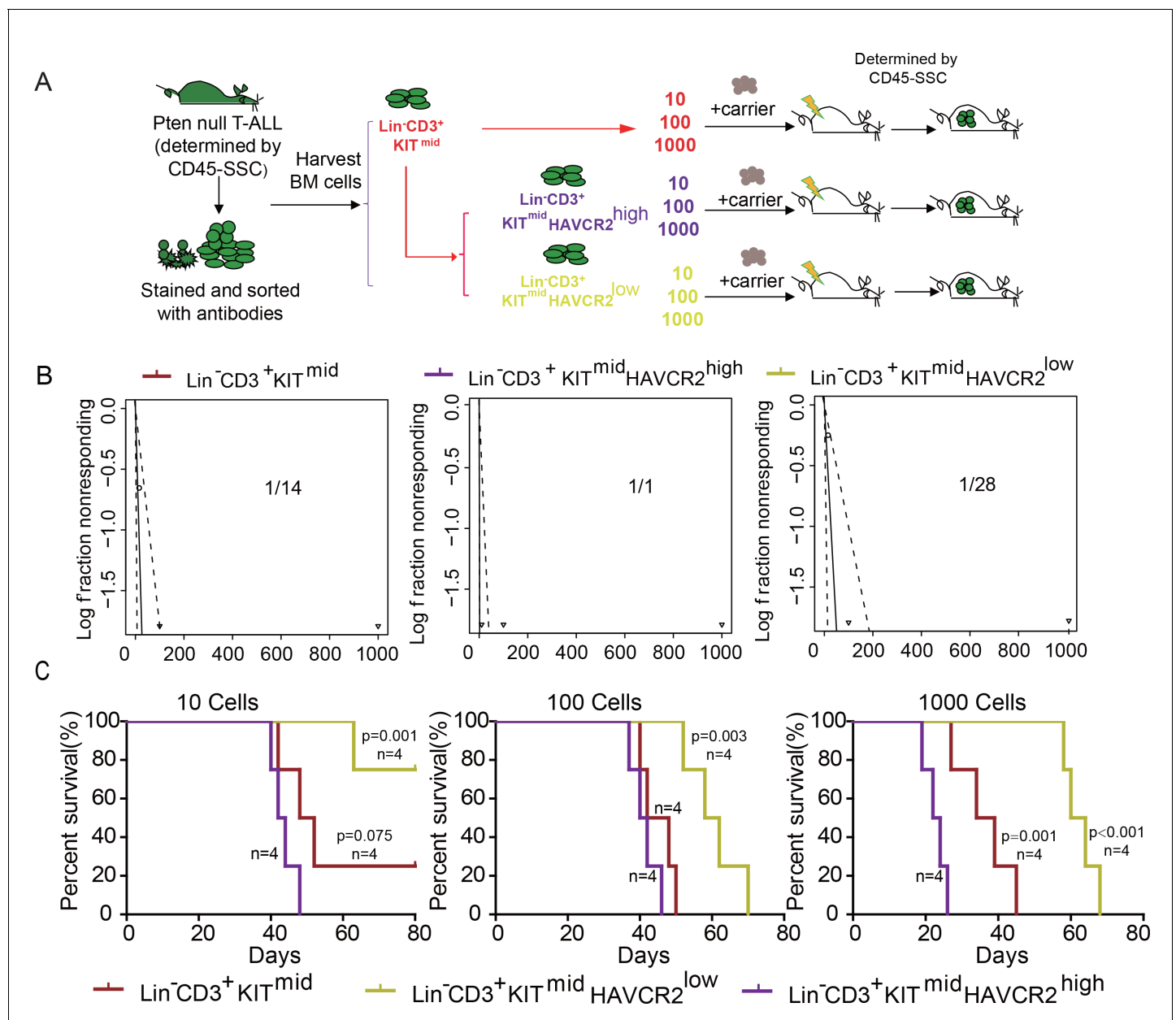


Figure 3. The HAVCR2^{high} subgroup contains the vast majority of LSC activity. (A) Schematic illustrating the cell isolation, limiting dilution and transplantation procedures used for testing LSC activity as described in Guo et al. (Guo et al., 2008); (B) LSC frequencies were calculated for each subgroup according to Hu et al. (Hu and Smyth, 2009); (C) Survival curves showing LSC activity in each of the sorted subgroups upon transplantation (n = 4). Student's t-test was used to calculate the p-value.

DOI: <https://doi.org/10.7554/eLife.38314.007>

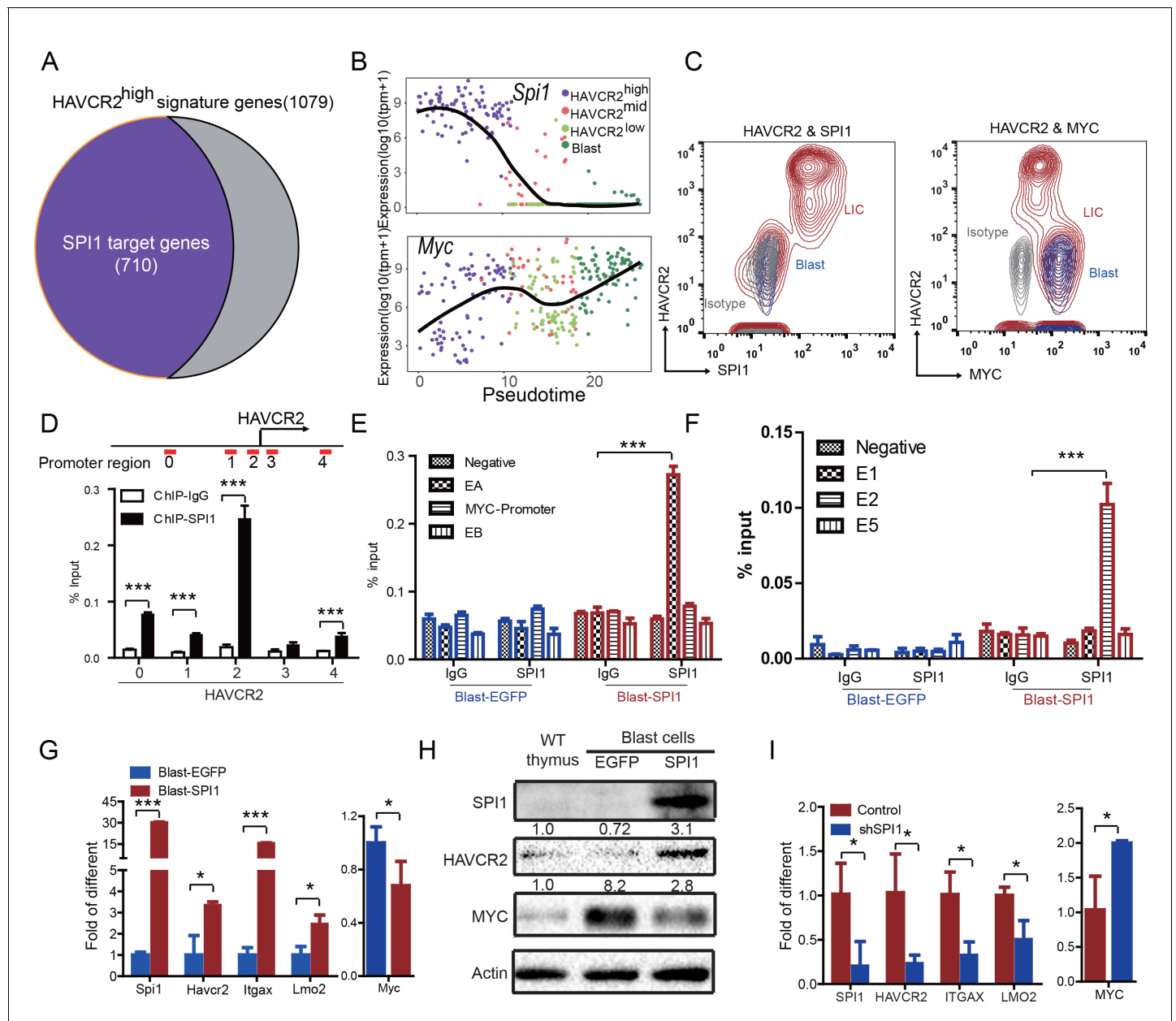


Figure 4. SPI1 is the master regulator of LSC signature genes and controls HAVCR2 and c-MYC expression. (A) Nearly 70% of the genes highly expressed in the HAVCR2^{high} subgroup—the LSC signature genes—are potential SPI1 target genes (purple); (B) Pseudotemporal ordering of single cells based on *Spi1* or *Myc* expression; (C) FACS analysis shows the correlation of HAVCR2 cell surface expression and intracellular SPI1 and c-MYC levels in the LSC-enriched (Lin⁺CD3⁺KIT^{mid}; red) and blast (Lin⁺CD3⁺KIT⁺; blue) subpopulations. Gray, isotype control; (D–E) ChIP-qPCR analysis identifies SPI1 binding regions in the HAVCR2 promoter (left) and *Tcra/d* enhancer A (EA) region (right), using Blast-SPI1 cells; (F) ChIP analysis identifies a SPI1 binding site in the endogenous *Myc* enhancer; (G) q-PCR shows the fold changes in *Havcr2*, *Itgax*, *Lmo2* and *Myc* expression between Blast-SPI1 cells (red) and Blast-EGFP cells (blue); (H) Western blotting shows the SPI1, HAVCR2 and c-Myc protein levels in WT thymus, Blast-EGFP and Blast-SPI1 cells. The fold changes relative to expression in the WT thymus are shown above each lane; (I) q-PCR analysis shows the fold changes in *HAVCR2*, *ITGAX*, *LMO2* and *MYC* expression in control shRNA (blue) and shSPI1 knockdown human T-ALL KE-37 cells (red); (D–I) All experiments were performed at least three independent times, and the data in D, E, F, G, and I are the means \pm S.Ds; * $p \leq 0.05$; ** $p \leq 0.01$; *** $p \leq 0.001$.

DOI: <https://doi.org/10.7554/eLife.38314.008>

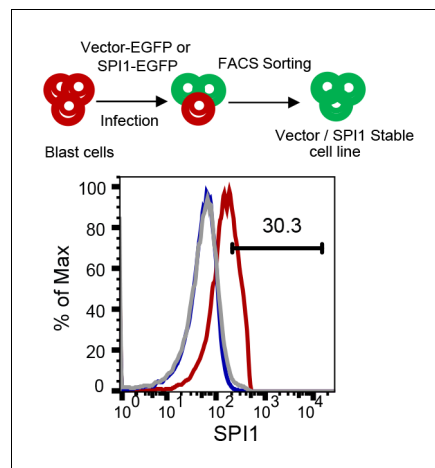


Figure 4—figure supplement 1. A schematic illustration of establishing lines expressing EGFP vector or EGFP-PU.1. Upper, a schematic illustration for establishing blast lines expressing the EGFP or EGFP-Spi1 vector; lower, FACS for intracellular SPI1 expression in blast cells infected with the empty EGFP retroviral vector (Blast-EGFP; blue) or the vector with EGFP-Spi1 cDNA (Blast-SPI1; red).

DOI: <https://doi.org/10.7554/eLife.38314.009>

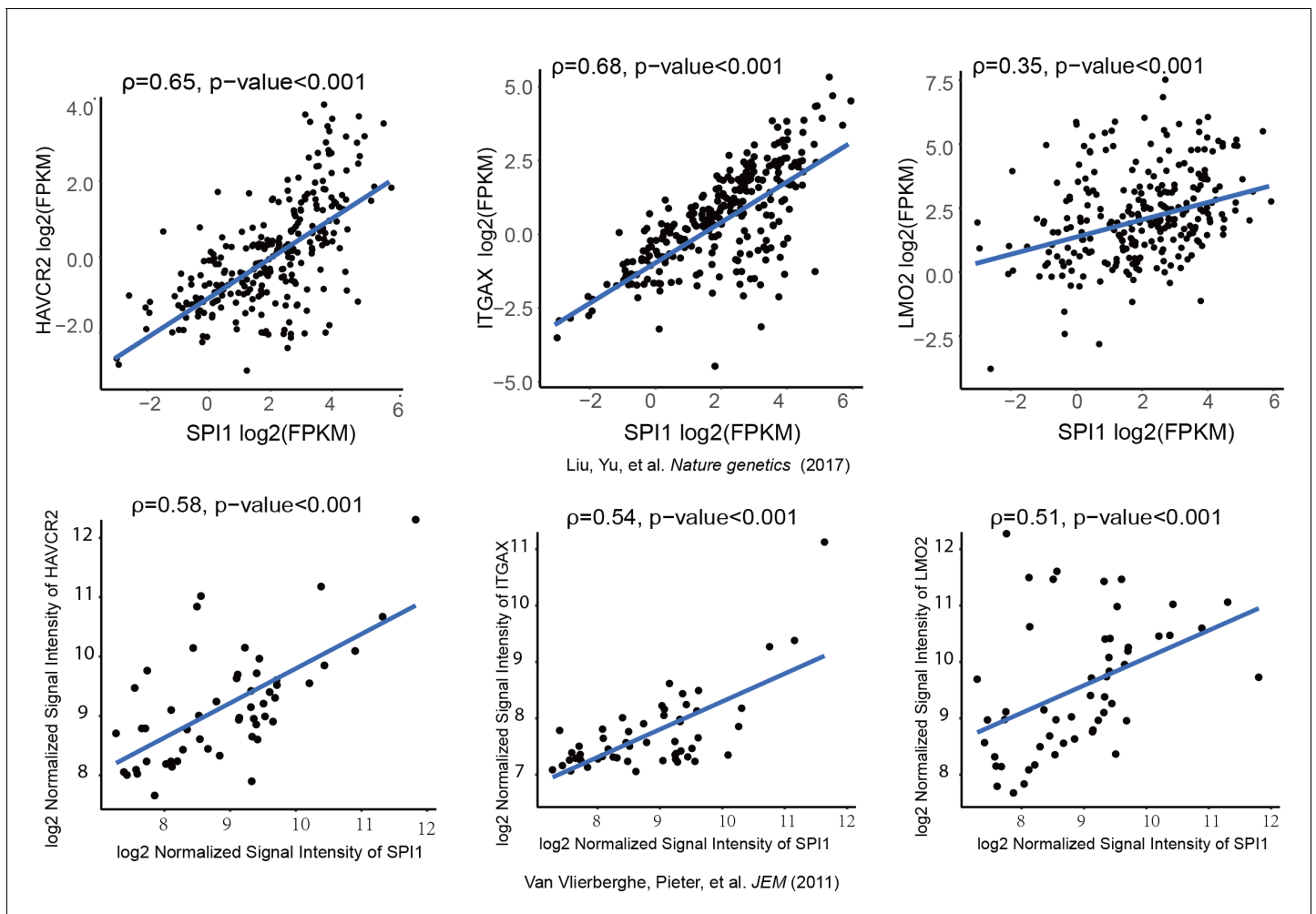


Figure 5. SPI1 expression is positively correlated with HAVCR2, ITGAX and LMO2 expression in human T-ALL. Correlation of SPI1 expression with HAVCR2, ITGAX and LMO2 expression in two different cohorts of human T-ALL samples, ρ : Spearman's rank correlation coefficient, p -value: p -value of Spearman's rank correlation test.

DOI: <https://doi.org/10.7554/eLife.38314.010>

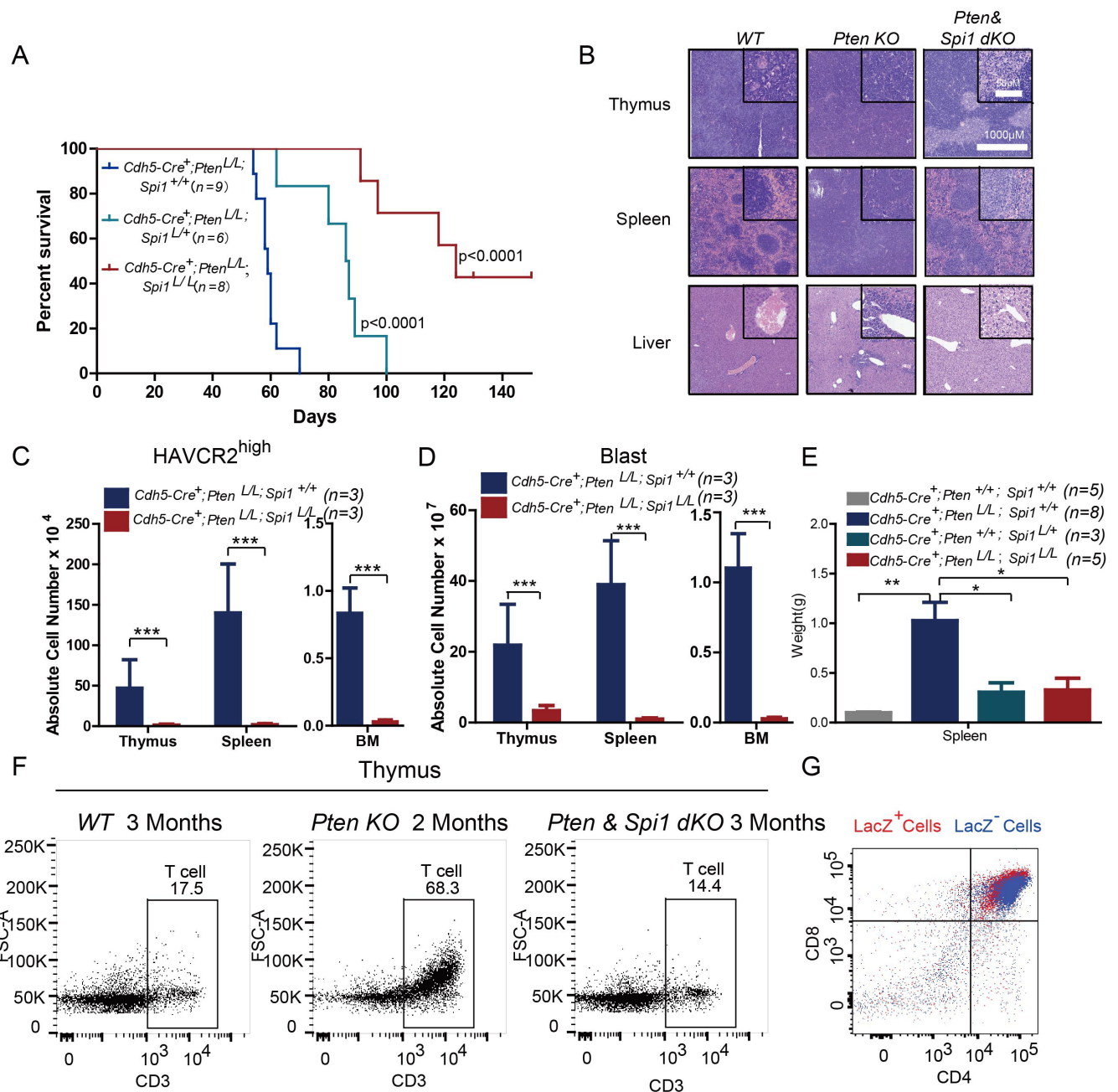


Figure 6. SPI1 is essential for LSC formation and T-ALL development. (A) Survival curves for *Cdh5-Cre⁺;Pten^{L/L}* T-ALL model mice (blue line) with heterozygous (*Cdh5-Cre⁺;Pten^{L/L};Spi1^{+/+}*; green line) or homozygous (*Cdh5-Cre⁺;Pten^{L/L};Spi1^{L/L}*; red line) *Spi1* conditional deletion; (B) HE-stained images of thymus, spleen and liver tissue from 2-month-old mice with the indicated genotypes; (C–D) Comparison of the absolute number of HAVCR2^{high} and blast cells in each organ in 2-month-old *Cdh5-Cre⁺;Pten^{L/L}* (blue bars) and *Cdh5-Cre⁺;Pten^{L/L};Spi1^{L/L}* (red bars) mice; (E) Comparison of spleen weights in the mice in B–C; (F) Representative FACS plots show CD3-positive T cells in the thymus of WT, *Pten*-null T-ALL and *Pten/Spi1* double knockout mice. WT and *Pten/Spi1* double knockout mice were 3 months old, and *Pten*-null T-ALL mice were 2 months old. n = 3; (G) FACS-Gal analysis of T cell development in the thymus of *Pten/Spi1* double knockout mice. LacZ⁺ cells (red dots) and LacZ⁻ cells (blue dots) from the same sample are overlaid. C–D, the data are presented as the means ± S.Ds; *p<0.05; **p<0.01; ***p<0.001. The bars in the HE images and inserts represent 1000 μm and 50 μm, respectively.

DOI: <https://doi.org/10.7554/eLife.38314.011>

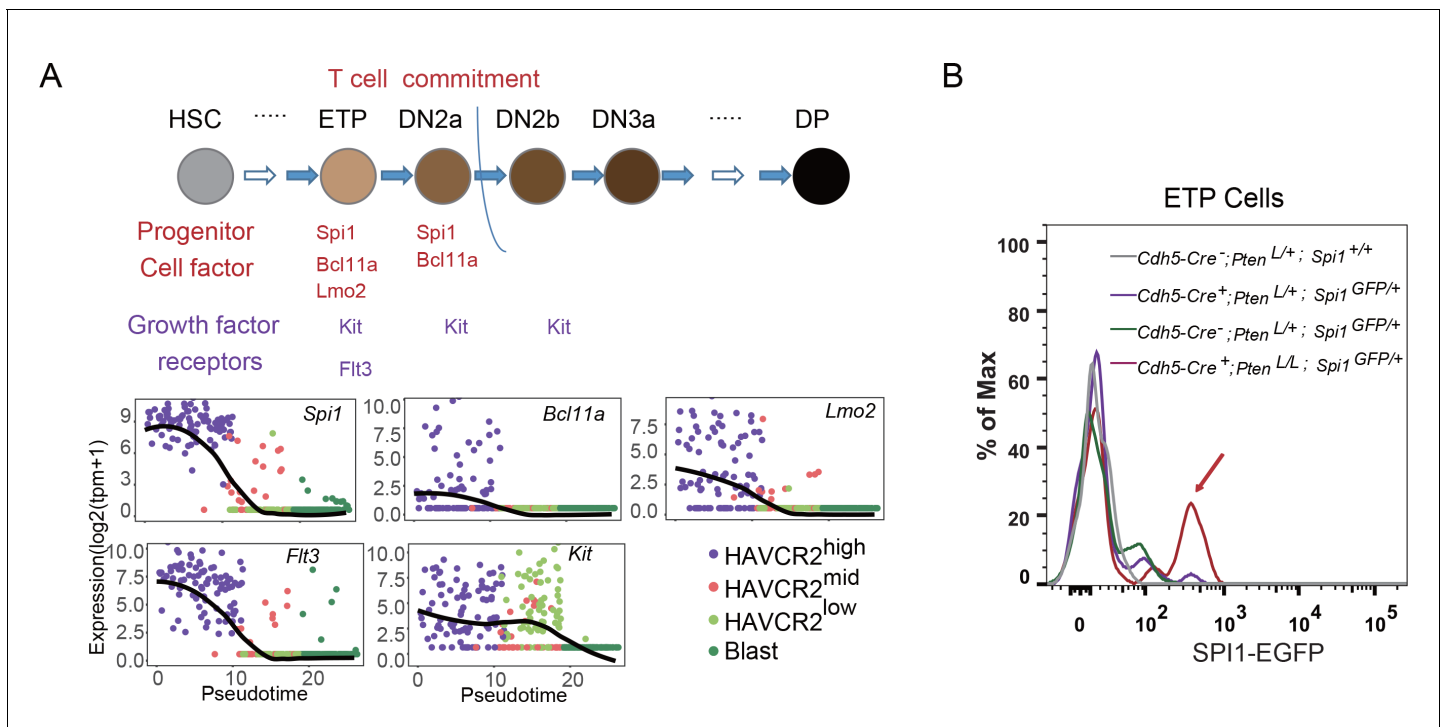


Figure 7. *Spi1* is upregulated at the ETP/DN1 stage during T cell development. (A) Upper panel: Diagram of progenitor cell factors and growth factor receptors involved in early T cell development, modified from (Rothenberg et al., 2016); lower panels: pseudotemporal ordering of single cells based on *Spi1*, *Bcl11a*, *Lmo2*, *Flt3* and *Kit* expression; (B) *Spi1*-GFP expression is upregulated in ETP/DN1 progenitor cells from *Cdh5-Cre⁺;Pten^{L/L}; Spi1^{GFP/+}* *Pten* null (red line), compared to that in *Cdh5-Cre⁺;Pten^{+/L}; Spi1^{+/+}* WT (gray line), *Cdh5-Cre⁺;Pten^{+/L}; Spi1^{GFP/+}* *Pten* heterozygous (purple line) and *Cdh5-Cre⁺;Pten^{+/L}; Spi1^{GFP/+}* WT GFP⁺ (green line) mice.

DOI: <https://doi.org/10.7554/eLife.38314.012>

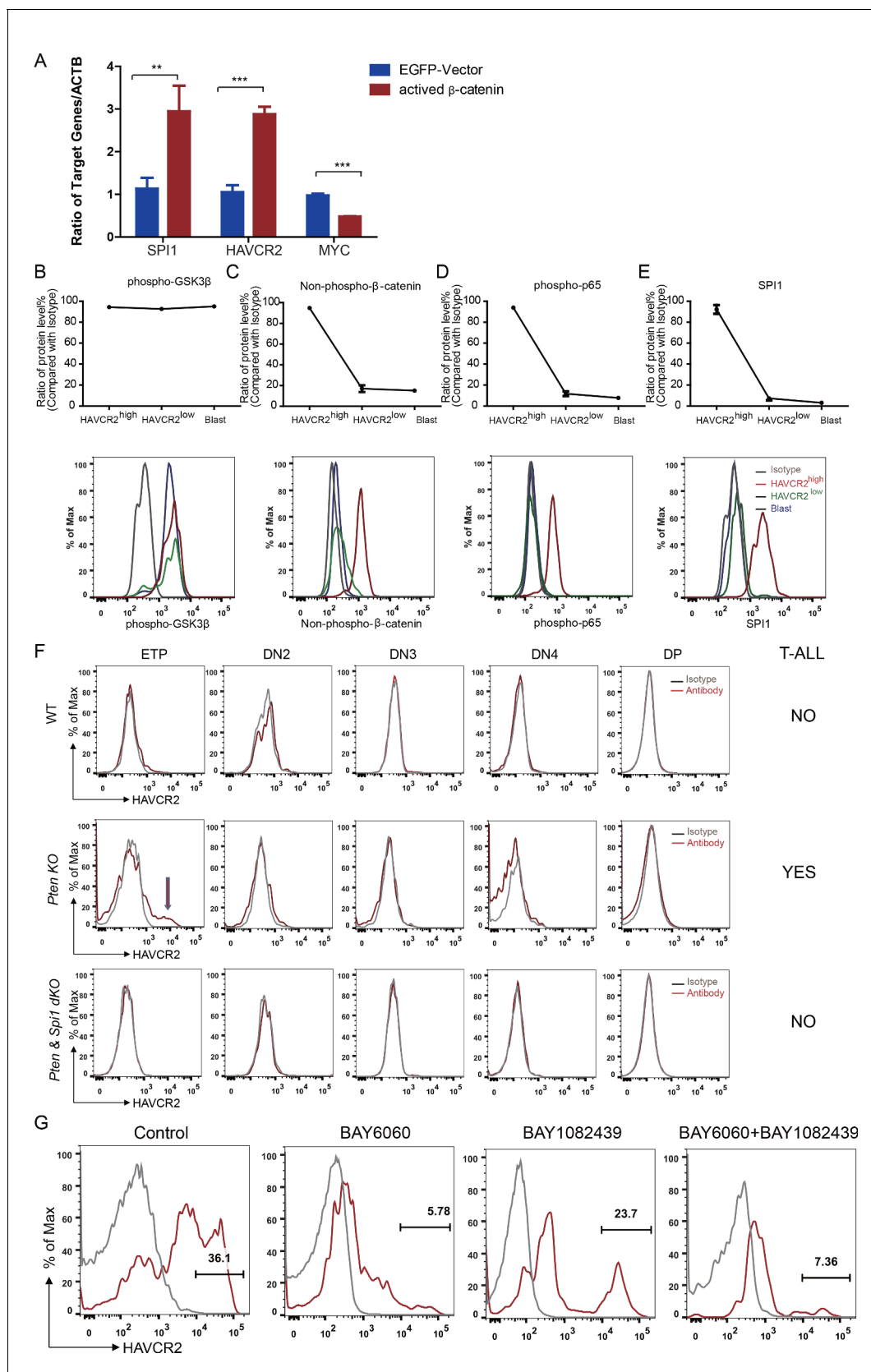


Figure 8. *Spi1* expression is maintained by β -catenin-SPI1-HAVCR2 regulatory circuit. (A) q-PCR analysis of SPI1 and SPI1-regulated HAVCR2 and c-MYC expressions after the overexpression of active β -catenin in the Jurkat T-ALL cell line (red bars). The data are normalized to that of empty plasmid

Figure 8 continued on next page

Figure 8 continued

controls (blue bars); (B–E) Upper panels: quantitative intracellular FACS analyses of P-GSK-3 β , non-phospho- β -catenin, P-p65 and SPI1 levels in the HAVCR2^{high}, HAVCR2^{low} and blast subgroups; lower panels: representative intracellular FACS analysis of P-GSK-3 β , non-phospho- β -catenin, P-p65 and SPI1 levels in the HAVCR2^{high}, HAVCR2^{low} and blast subgroups. Gray line, isotype control; (F) FACS analysis shows cells in the HAVCR2^{high} subgroup at the ETP/DN1 stage, which are absent in WT and dKO mice; (G) Representative FACS plots show the number of cells in the HAVCR2^{high} subgroup in the different drug treatment groups. The data in A, B, C, D and E are the means \pm S.Ds of 3 independent tests; * $p \leq 0.05$; ** $p \leq 0.01$; *** $p \leq 0.001$.

DOI: <https://doi.org/10.7554/eLife.38314.013>

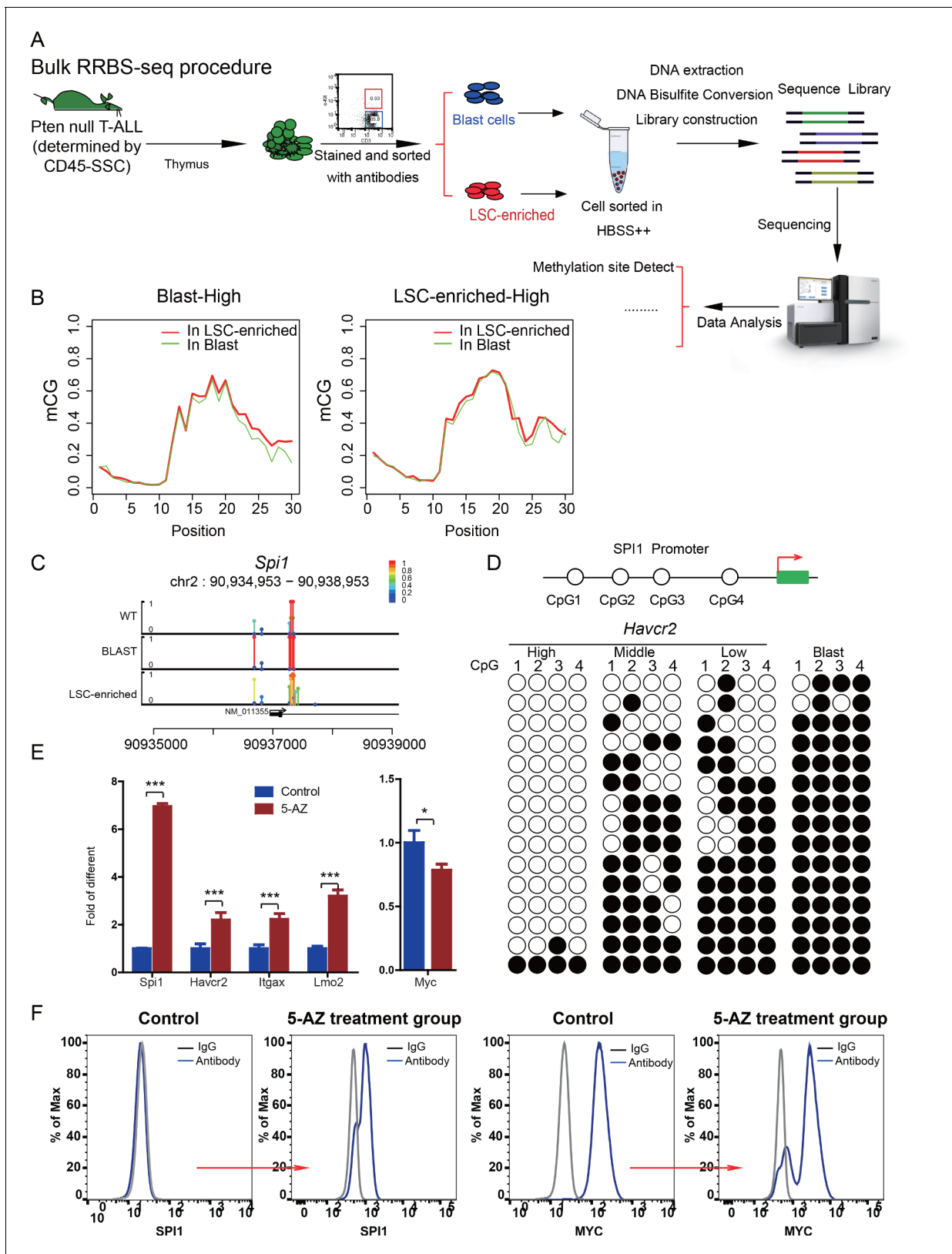


Figure 9. *Spi1* expression is controlled by DNA methylation (A) Schematic illustrating the procedures involved in cell isolation and RRBS analysis; (B) DNA methylation status of genes specifically expressed in the leukemic blast (left) and LSC-enriched (right) subpopulations; (C) *Spi1* promoter methylation status in normal T cells, LSC-enriched cells and blast-enriched cells.

DOI: <https://doi.org/10.7554/eLife.38314.014>

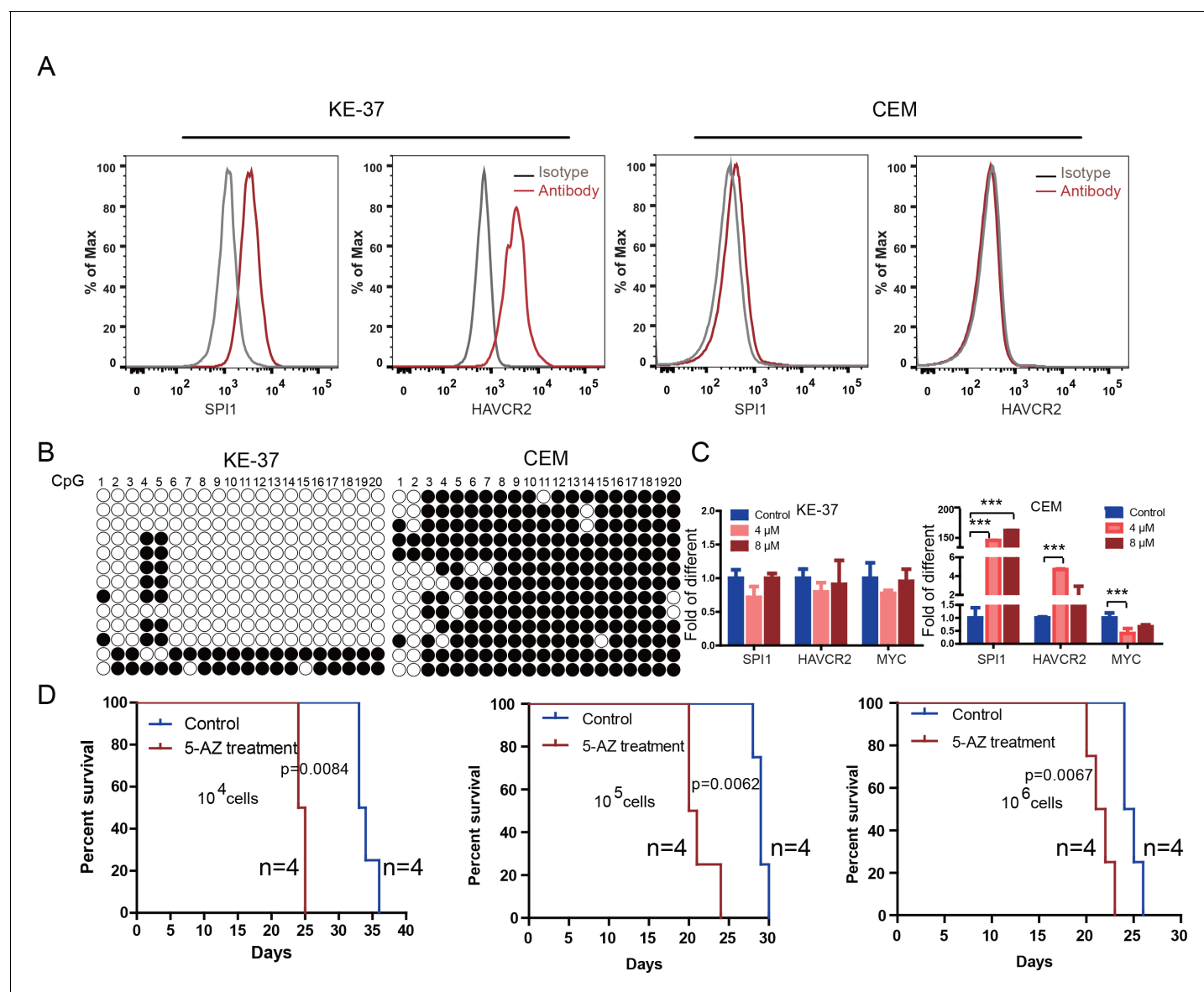


Figure 10. Human *SPI1* expression is silenced by DNA methylation (A) FACS analysis shows the surface expression of HAVCR2 and the intracellular level of SPI1 in the human T-ALL cell lines KE-37 and CEM.(B) Methylation status of CpG islands in the *SPI1* promoter in the human T-ALL cell lines KE-37 and CEM; (C) q-PCR analysis of *SPI1*, *HAVCR2* and *Myc* expression in KE-37 and CEM cells without (blue) and with (pink and red) 5-AZ treatment *in vitro*; (D) Survival curves show T-ALL development by CEM cells without (blue) and with (red) 5-AZ treatment upon transplantation (n = 4; t-test). The data in Care the means \pm S.D.s of 3 independent tests; * $p \leq 0.05$; ** $p \leq 0.01$; *** $p \leq 0.001$.

DOI: <https://doi.org/10.7554/eLife.38314.015>

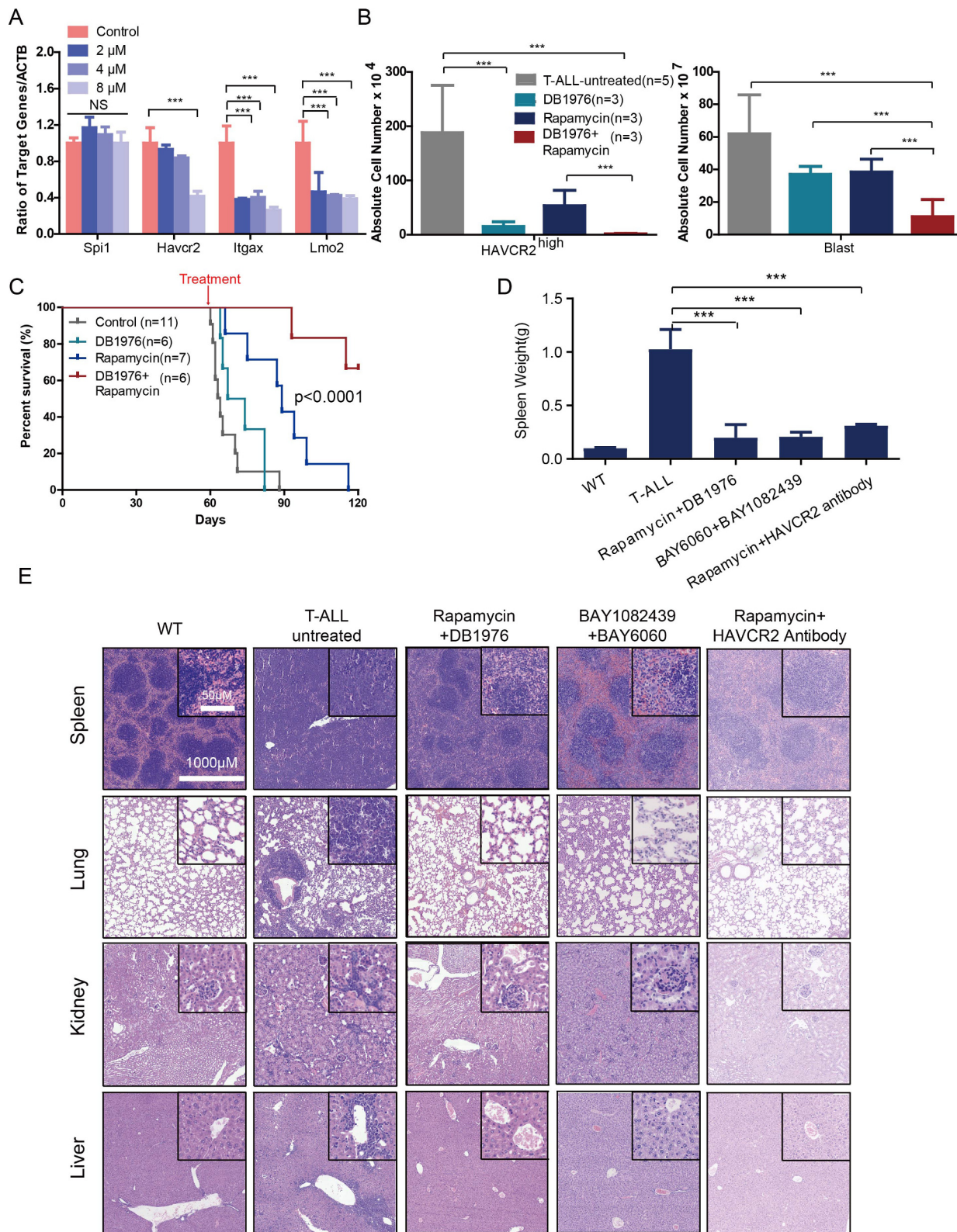


Figure 11. Cotargeting oncogenic driver mutations and the LSC 'stemness' maintenance circuit eliminated LSC and T-ALL cells (A) q-PCR analysis of *Spi1* and *Spi1*-regulated *Havcr2*, *Itgax* and *Lmo2* expression after 24 hr of DB1976 treatment (blue bars). The data are normalized to that of the

Figure 11 continued on next page

Figure 11 continued

untreated controls (red bars); (B) A comparison of the absolute number of HAVCR2^{high} and blast cells in the untreated (gray bars) and differently treated groups; (C) Survival curve of *Cdh5-Cre⁺;Pten^{L/L}* model mice treated with DB1976 and rapamycin alone and in combination; (D) A comparison of the spleen weights of 2-month-old WT mice, untreated *Cdh5-Cre⁺;Pten^{L/L}* mice, and combination-treated mice upon euthanasia; (E) HE-stained images of spleen, lung, kidney and liver tissue from 2-month-old WT, untreated and combination-treated mice. A, B and D: the data are presented as the means \pm S.Ds; *** $p \leq 0.001$; the bars in the HE images and inserts represent 1000 μ M and 50 μ M, respectively.

DOI: <https://doi.org/10.7554/eLife.38314.016>

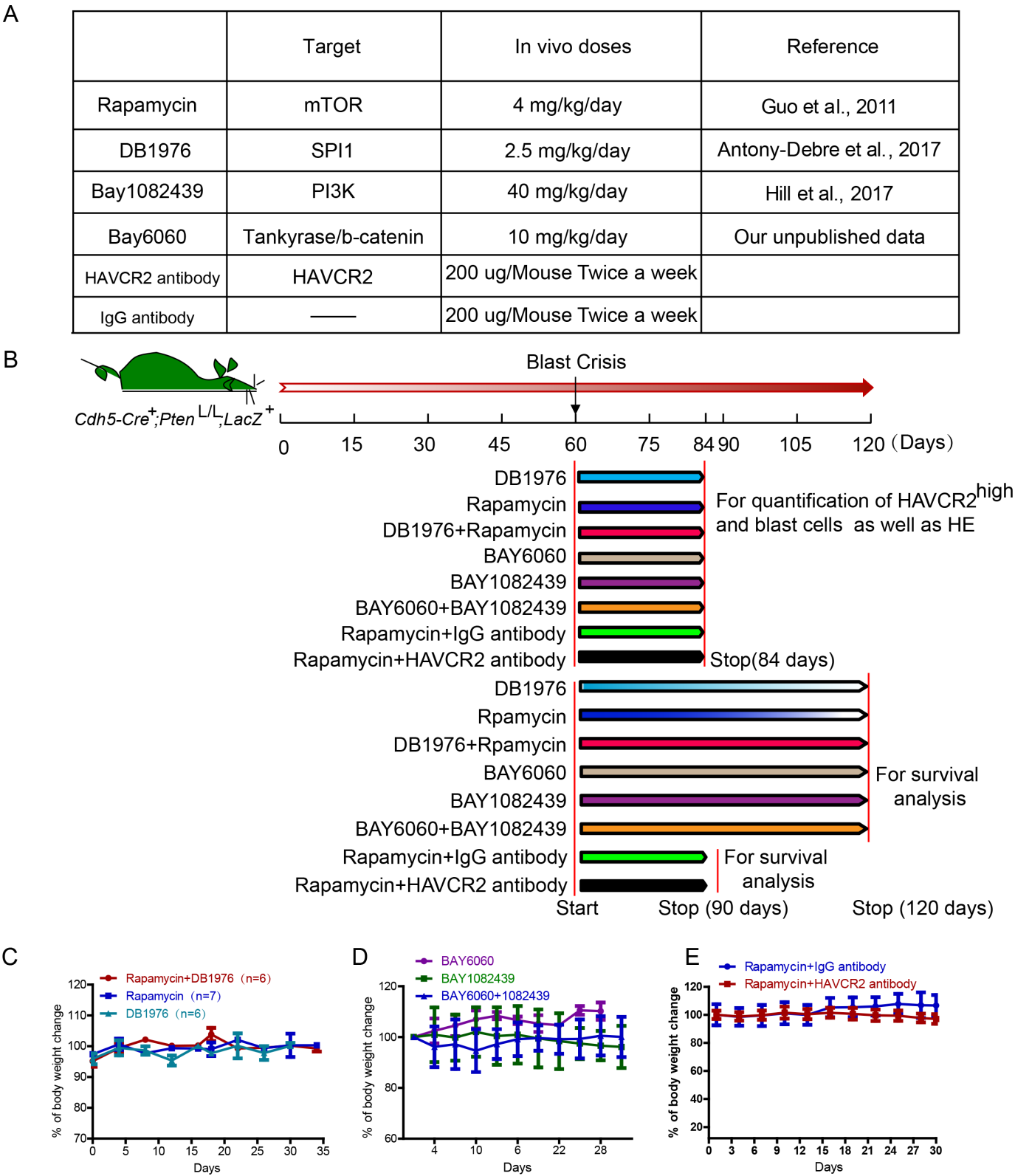


Figure 11—figure supplement 1. A schematic illustration of dosing schedules and treatment cohorts. (A) Table showing all inhibitors used in this study, including their targets, *in vivo* dosages and references. (B) Schematic illustration of the different treatment cohorts and analyses; (C– E) Lack of general body weight loss in each treatment cohort.

DOI: <https://doi.org/10.7554/eLife.38314.017>

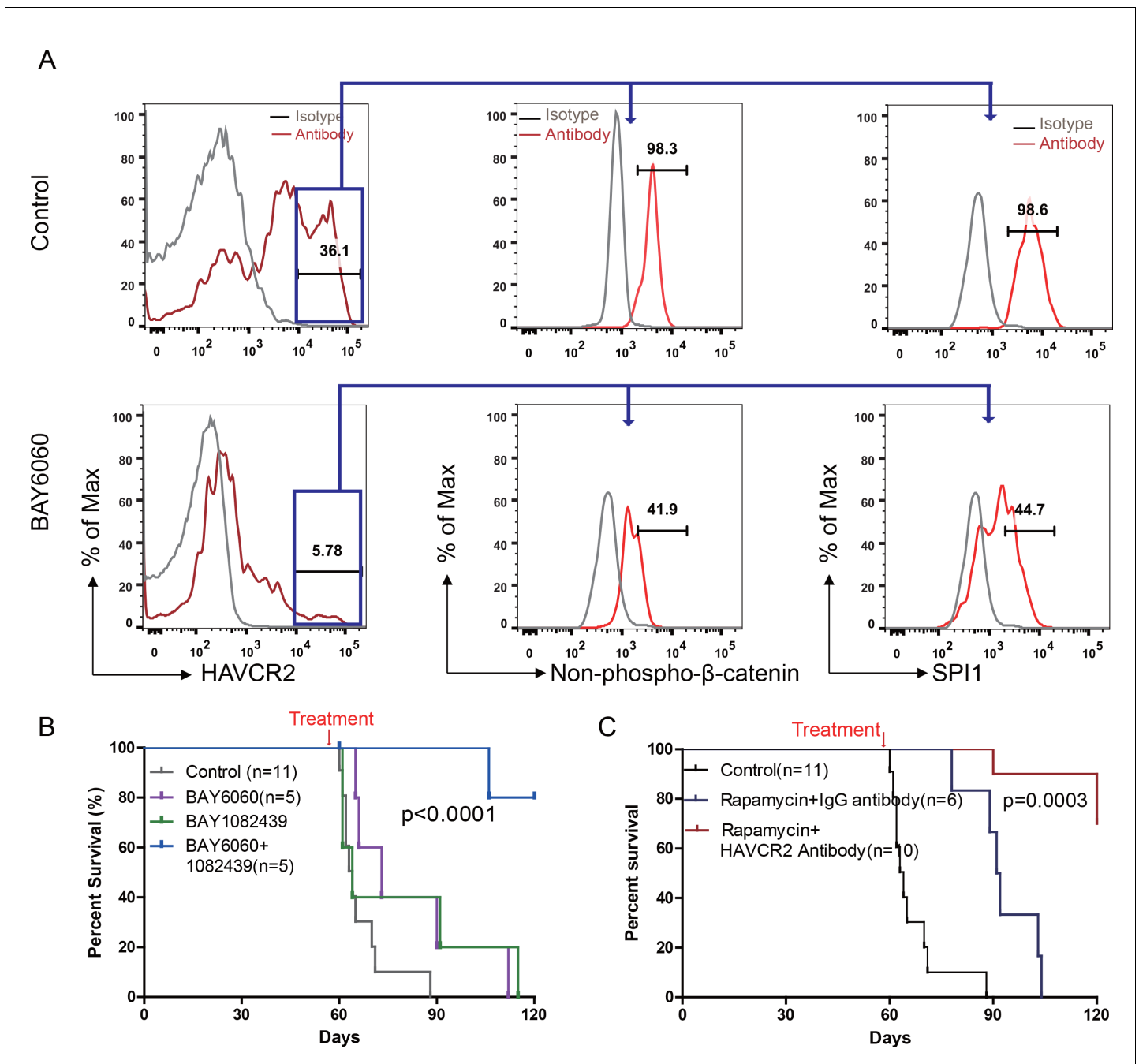


Figure 12. Cotargeting oncogenic driver mutations and LSC 'stemness' maintenance circuit. (A) Comparison of the HAVCR2^{high} subgroup population (left panel) and of the levels of non-phosphorylated β -catenin (middle panel) and SPI1 (right panel) within the HAVCR2^{high} subgroup without (upper panels) and with BAY6060 treatment (low panels); (B) Survival curve for *Cdh5-Cre⁺;Pten^{L/L}* mice treated with BAY6060 and BAY1082439 alone and in combination; (C) Survival curve for *Cdh5-Cre⁺;Pten^{L/L}* mice treated with rapamycin in combination with either an IgG control antibody or an anti-HAVCR2 antibody.

DOI: <https://doi.org/10.7554/eLife.38314.018>

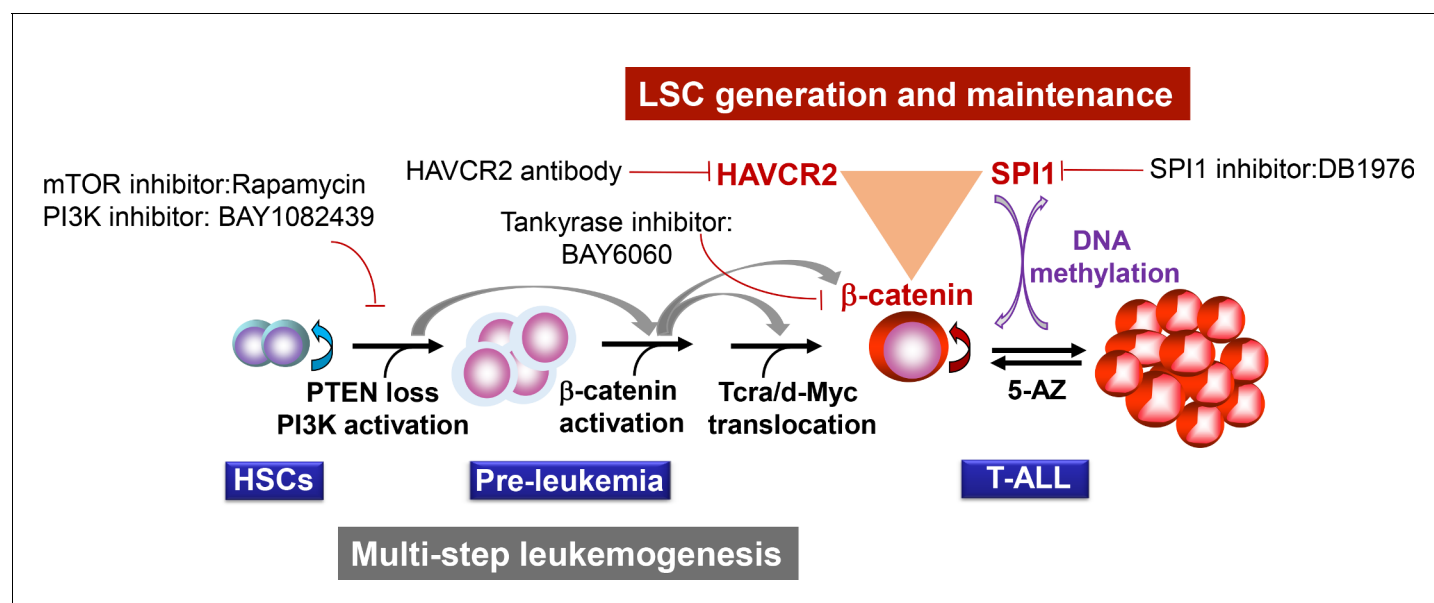


Figure 13. Two-layer control mechanisms for leukemogenesis and LSC maintenance.

DOI: <https://doi.org/10.7554/eLife.38314.019>